

Bio-electrocatalysis of *Acetobacter aceti* through direct electron transfer using a template deposited nickel anode

Rengasamy Karthikeyan, V. Ganesh and Sheela Berchmans*

Received 14th January 2012, Accepted 27th February 2012

DOI: 10.1039/c2cy20022h

We have developed a novel anode for microbial fuel cells (MFC) which exhibits effective direct electron transfer with *Acetobacter aceti*. A high surface area nickel electrode was obtained using a simple process of template electrodeposition and it significantly improved the bioelectrocatalytic activity of *Acetobacter aceti* towards the oxidation of ethanol and glucose. Electrodeposition of Ni on carbon paper was carried out in the absence and presence of a soft template which served as the substrate for direct electron transfer. The soft template consists of a two component mixture of Triton X-100 and water. The structural and morphological characterizations of these modified electrodes were carried out using scanning electron microscopy (SEM). The redox properties of the biofilm formed on Ni coated carbon electrodes were investigated using cyclic voltammetry (CV) and chronoamperometry (CA). The formation of redox peaks during CV studies suggests the presence of a membrane bound redox protein linked to pyrroloquinoline quinone (PQQ) within these microbes on the modified electrodes. Investigation of the scan rate dependence reveals that the proteins are surface confined and anchored. From CA studies, we found that the oxidation current density corresponding to glucose and ethanol was more for the template deposited nickel (TNiCP) when compared to the one without the template. The oxidation current density of ethanol was found to be higher ($68 \mu\text{A cm}^{-2}$ i.e., 680 mA m^{-2}) in comparison to glucose ($42 \mu\text{A cm}^{-2}$ i.e., 420 mA m^{-2}). For comparison, we have also carried out all these studies using a bare carbon paper (CP). Our results clearly demonstrate the direct electron transfer between *Acetobacter aceti* and high surface area nickel electrodes through the membrane bound redox enzyme which presumably contributes to the higher oxidation current density of ethanol and glucose and could be used as an alternative anode material for MFC applications.

1. Introduction

Microbial fuel cells (MFC) are an upcoming green technology that can provide electricity from degradable waste components by the catalytic oxidation using microorganisms. This technology has several potential applications in the field of bio-remediation, wastewater treatment and bioenergy.^{1,2} In order to explore the extracellular electron transfer mechanisms in mixed as well as pure cultures, the study of energy metabolism under the controlled redox conditions and microbial physiology is essential.³ Microorganisms can donate electrons to the anode most commonly through two processes namely, (i) direct electron transfer (DET) through either c-type cytochromes or conductive pili and (ii) mediated electron transfer (MET) using (redox) mediators. However MET will not be suitable for practical applications and the research interest has been diverted to the development

of exoelectrogens that are capable of performing a direct electron transfer process.⁴ Numerous studies have been carried out using the genera *Geobacter* and *Shewanella* in order to elucidate the electrochemical activity of their biofilm. Moreover the performance of the anode depends mainly on the density of biofilm grown on that substrate and its ability to oxidize a fuel effectively using the redox properties of membrane bound enzymes present within the biofilm.

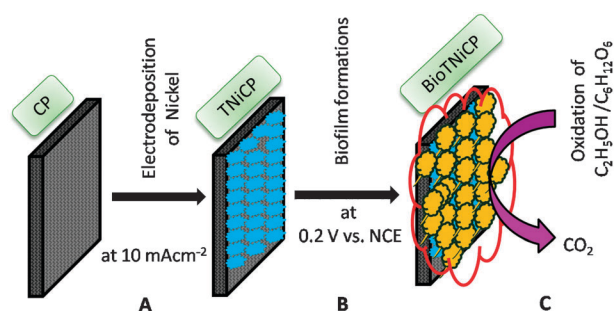
The electroactivity of the biofilm depends upon the anode materials. A few of the new materials explored as anodes for MFC are carbon nanotubes/polyaniline,⁵ titanium dioxide/polyaniline,⁶ and mediator immobilized carbon.⁷ The electrochemical behavior of a metal reducing bacterium (*Geobacter sulfurreducens*) formed on a graphite electrode was investigated under poised potential and an oxidation current density of $75 \mu\text{A cm}^{-2}$ for 10 mM acetate as a fuel was reported.⁸ The biofilm of *Geobacter* sp., formed on a carbon paper was found to produce a higher oxidation current density of $1358 \mu\text{A cm}^{-2}$ for 10 mM acetate that has been used as a fuel when compared to that of other materials such as graphite rods, polycrystalline carbon rods, carbon fiber veil, graphite foil, polycrystalline

Electrodeposition and Electrocatalysis (EEC) Division,
Central Electrochemical Research Institute (CSIR-CECRI),
Karaikudi-630 006, Tamilnadu, India.
E-mail: sheelaberchmans@yahoo.com; Fax: +91-4565-227779;
Tel: +91-4565-241241 and 241251

carbon rods and glassy carbon rods.⁹ Similarly, immobilization of *Shewanella* sp. onto a graphite felt electrode was found to produce a current density of $0.6 \mu\text{A cm}^{-2}$ for 10 mM lactate oxidation reaction and it was realized that the presence of a localized decaheme namely, c-Cyts OmcA and MtrC, on the surface of a cell is responsible for transferring the electron to the graphite felt electrode.¹⁰ By interfacing inoculums of heat treated soil with an electrocatalyst like tungsten carbide, WC, Rosenbaum *et al.* reported a maximum current density of 3.0 mA cm^{-2} for the oxidation of 5 g L^{-1} glucose,¹¹ which is considered to be the maximum oxidation current density value reported for an MFC before 2010. In addition, a multi-walled carbon nanotubes (MWNTs) incorporated glassy carbon electrode was also found to be a promising material for promoting the direct electron transfer process. Using this electrode, an oxidation current density of $9.7 \mu\text{A cm}^{-2}$ was reported by employing *Shewanella oneidensis* as the microorganism using Luria–Bertani (LB) broth (Difco Laboratories, MI, USA).⁴ Hence much more attention has been paid to three dimensional (3D) carbon materials. In this direction, an electrospun carbon fiber mat with a layered architecture was employed as an anode by anchoring a biofilm of mixed culture obtained from Braunschweig waste-water treatment plant that produced an oxidation current density of 2.0 mA cm^{-2} for 10 mM acetate and the reason for obtaining this much higher current density was attributed to the formation of a high density biofilm.¹²

Pyrroloquinoline quinone (PQQ) containing enzymes have been found in different species and were found to be responsible for the dehydrogenation of alcohols or sugars.¹³ Among them PQQ dependent alcohol dehydrogenase (ADH) is rather unique and exhibits interesting properties depending on the bacterial species and found to be located usually in the periplasmic fraction. *Acetobacter aceti* belongs to the group of acetic acid producing bacteria containing PQQ dependent ADH protein as a membrane fraction. It consists of a characteristic active respiratory chain which can oxidize several alcohols, sugars and sugar alcohols. Their corresponding oxidized products are accumulated in the culture medium itself.^{14,15} Moreover PQQ–ADH has potential applications in biotechnology as well as fuel cells for direct and indirect electron transfer processes.¹⁶ Our previous studies have shown the possibility of direct electron transfer occurring between the biofilm of mixed culture (*Acetobacter aceti* and *Gluconobacter roseus*) immobilized onto a glassy carbon electrode. The redox activity of such biofilm mainly arises from the presence of a membrane bound enzyme (ADH complexed with cytochrome C). It is well known that direct electron transfer of the biofilm for a mediator-less MFC could be enhanced by the electrochemical redox activity of different base materials or a chemically modified anode as a base material without the assistance of an external mediator.¹⁷ The electrochemical half cell studies are one of the key approaches to characterize the electrode in an MFC and are also helpful to interpret the mechanism of electron transfer between anode and bacteria.^{4,18}

In the present work, we mainly focus on the performance of a half-cell microbial anode using different electrodes namely bare carbon paper (CP), nickel deposited carbon paper (TNiCP) using a template and nickel deposited carbon paper (NiCP) without a template (see Scheme 1). *Acetobacter aceti* is



Scheme 1 Schematic illustration of the electrode modification process and biofilm formation. (A) Electrodeposition of Ni on CP using a template/non template medium at a constant current density of 10 mA cm^{-2} , (B) poising of the anode potential for biofilm formation using the microorganism *Acetobacter aceti*, (C) bioelectrocatalysis of glucose or ethanol.

used for biofilm formation. The biofilm is formed on the above mentioned electrodes under a poised potential of 0.2 V vs. NCE (normal calomel electrode) and the bio-electrochemical oxidation ability is assessed in the presence of electron donors namely glucose and ethanol. Electrochemical activity of such an immobilized biofilm is investigated using cyclic voltammetry (CV) and chronoamperometry (CA). The structural, morphological and surface characterizations of biofilm modified electrodes are carried out using scanning electron microscopy (SEM). Here, we report for the first time, the biofilm (of *Acetobacter aceti*) formation on a novel template based nickel modified carbon paper which exhibits higher electroactive moieties per unit area compared to biofilms on unmodified carbon paper. The electron transfer rate constants of the biofilms and the bioelectrocatalytic activity are found to be higher on the template based nickel modified carbon paper. A novel template deposited nickel electrode effectively tunnels the electrons from *Acetobacter aceti* and establishes direct electrical communication between the electrode and the microorganism.

2. Materials and methods

2.1. Chemicals

Nickel chloride (Riedel-de Haen), boric acid (Sisco), nickel sulfamate (Grauer & Weil India Ltd.), Triton X-100 (SD fine chemicals), sodium hydroxide (Merck), hydrochloric acid (Fischer Scientific chemicals), acetone (Fischer Scientific chemicals), hydrogen peroxide (Ranbaxy), glucose (Sigma Aldrich) and ethanol (Merck) were used in this study. All these chemicals were used as received unless otherwise stated. Carbon paper (E-TEK) was used as strips and as a working electrode for electrodeposition of nickel. All the aqueous solutions were prepared using Millipore water obtained from the quartz distillation unit having a resistivity of $18 \text{ M}\Omega \text{ cm}$.^{18,19}

2.2. Modification of carbon paper with nickel electrodeposits

A piece of carbon paper with a geometrical area of 0.5 cm^2 ($0.5 \text{ cm} \times 0.5 \text{ cm} \times 2$ —for both sides) was used for the electrodeposition of nickel. The electrical connection was made with a brass rod using a proper sealing. The fabricated carbon paper electrodes were cleaned with acetone by sonicating them for about 5 minutes followed by cleaning using Millipore water.

Electrodeposition of Ni was carried out using a nickel sulfamate bath consisting of 300 g L⁻¹ nickel sulfamate, 6 g L⁻¹ nickel chloride and 30 g L⁻¹ boric acid. In order to investigate the template assisted electrodeposition, Triton X-100 was used along with the nickel sulfamate bath, the combination of which is known to form a hexagonal lyotropic liquid crystalline phase that can act as a template for electrodeposition of nickel.²⁰ A sulfurized nickel bar was used as an anode. Electrochemical deposition of Ni on carbon paper was performed cathodically by applying a constant current density of 10 mA cm⁻² for about an hour. After that the electrodeposited carbon paper electrodes were washed with plenty of distilled water to completely remove the template molecules and then immediately used for further studies and analysis.

2.3. Bio-electrochemical experiments

The half cell studies on CP and nickel deposited CPs using a template and without a template were carried out by employing glucose and ethanol as electron donors. In addition similar experiments were also performed using biofilm grown on these electrodes by utilizing *Acetobacter aceti* as a biocatalyst. All bioelectrochemical experiments were carried out by using a three-electrode setup consisting of the carbon paper electrode as a working electrode (anode), Hg/Hg₂Cl₂ (normal calomel electrode, NCE, 1 N KCl) as a reference electrode and Pt-foil as a counter electrode under anaerobic conditions at 28–30 °C. Phosphate buffer (pH 7, 25 ml) was used as a supporting electrolyte. The biocatalyst *Acetobacter aceti* (NCIM No. 2116) used in this study was procured from NCL, Pune, India. The sub-culturing of *Acetobacter aceti* was carried out by using a standard media composition of tryptone 1 g, yeast extract 1 g, glucose 1 g, CaCO₃ 1 g in 100 ml of distilled water. After the incubation period of about 48 h the cells were centrifuged at 8000 rpm at -20 °C in a refrigerated centrifuge (RC4100F, Promega instruments private limited) and the pellet (0.3 g) was used as inoculum to form an electroactive biofilm on the electrodes. The biofilm was grown by poisoning the working electrode at a constant potential of 0.2 V vs. NCE and the current response was collected using a data acquisition unit (Agilent acquisition 34970A data acquisition/switch unit). In order to describe the electrocatalytic and bio-electrocatalytic effects, initially the oxidation current was recorded with only a fuel alone (abiotic process) and allowed to reach the steady state current. After that the biofilm formation was carried out using culture inoculums leading to attainment of the bacterial lag period. At this point the reactor solution was replaced by a fresh phosphate buffer medium (pH 7) containing either 25 mM glucose or ethanol (biotic process) and the oxidation current was monitored simultaneously. Cyclic voltammetry (CV) of the biofilm formed electrodes was carried out before and after the chronoamperometry studies during which the working electrodes were gently removed from the reactor and washed with phosphate buffer. CVs were recorded using a PGSTAT 302N (Autolab systems; Ecochemie) electrochemical system and the data were analyzed using General Purpose Electrochemical Software (GEPS) provided by them.

2.4. SEM analysis

Surface characterization of such modified and biofilm immobilized carbon paper electrodes was carried out using SEM.

These electrodes were used as strips for the analysis. The biofilm anchored electrodes were removed from the reactor and washed with phosphate buffer (pH 7). Then the electrodes were stained with 50 µl of 0.1% phosphotungstic acid and gradually dehydrated with acetone 50%, 70%, 100% solutions and finally the electrodes were used for imaging using SEM (Hitachi S-3000N model).

3. Results and discussion

3.1. Surface characterization of template deposited Ni on carbon paper

Electroplating of Ni on CP was initially confirmed by visualization as it is evident from the color change of black for CP to grey for nickel deposited CP. Further SEM was used for the structural and morphological characterization of the Ni deposits on CP and the corresponding SEM images are shown in Fig. 1. For comparison the SEM picture of bare CP without the Ni deposit is also provided. It can be seen from these figures that bare CP shows the network of fiber structures that are thin and long in dimension. In addition, it also exhibits pores in between these fibers. In contrast, Ni deposited CP displays a dense homogeneous film formation within these fibers in the absence of a template and aggregates of Ni particles with porous structures in the case of template deposition. Lower magnification images of the template deposited Ni exhibit the Ni particles to be smaller with clear grain boundaries. Moreover they also display fractal

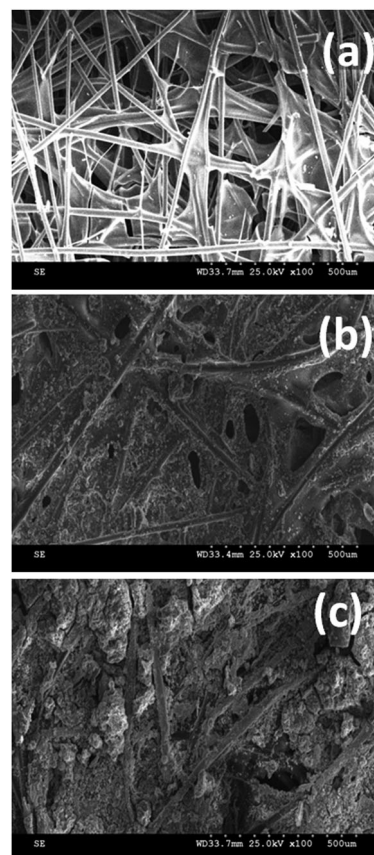


Fig. 1 SEM pictures of CP (a), NiCP (b) and TNiCP (c) electrodes before biofilm formation.

growth with pores suggesting the possibility of high surface area for these materials.

3.2. Biofilm formation on Ni deposited CP

Initially cyclic voltammetry (CV) experiments were carried out to assess the quality of biofilm formation using an aqueous solution of phosphate buffer as an electrolyte at a potential sweep rate of 50 mV s^{-1} . The cyclic voltammograms of CP (a) and TNiCP (b) electrodes before and after the biofilm formation are shown in Fig. 2. It can be seen from these CVs that both the electrodes after the biofilm formation show a distinct redox peak formation in comparison to the one before biofilm formation.

The appearance of a redox peak is very clear and pronounced in the case of biofilm grown on TNiCP when compared to the biofilm grown on CP where we observed a small peak formation. Interestingly, biofilm of *Acetobacter aceti* on CP showed a well defined single redox peak with midpoint potential of 0.064 V (where $E_{\text{pa}} = 0.12 \text{ V}$ and $E_{\text{pc}} = 0.008 \text{ V}$), which is very close to the values obtained for the same biofilm grown on NiCP (0.07 V) and TNiCP (0.09 V) respectively. This clearly indicates the presence of a membrane bound redox enzyme (PPQ) within the immobilized biofilm on these electrodes. Further, the surface coverage of electroactive groups in the biofilm formed on these electrodes was calculated by measuring the charge integral under the redox peak using the following equation.

$$\Gamma = Q/nFA \quad (1)$$

where Γ is the surface coverage value, Q is the charge measured under the redox peak, n is the number of electrons, F is the Faraday constant and A is the area of electrode. We have determined the coverage of electroactive moieties per unit area as $2.902 \times 10^{-10} \text{ mol cm}^{-2}$ for CP, $7.3763 \times 10^{-9} \text{ mol cm}^{-2}$ for TNiCP and $4.3023 \times 10^{-9} \text{ mol cm}^{-2}$ for NiCP respectively.²¹ It is clear from these values that the surface coverage of the electroactive moieties in the biofilm follows the order: TNiCP > NiCP > CP. We also found that the density of electroactive groups present in the biofilm in the case of the TNiCP electrode is 25 times higher (more electro-active moieties per unit area) than the CP and 2 times higher than that of the NiCP electrode.

Scan rate dependence on the redox behaviour observed for the biofilm growth on these electrodes was also investigated. These studies were carried out for various scan rates from 10 mV s^{-1} to 50 mV s^{-1} and the corresponding CVs are displayed in Fig. 3. We have shown the CVs of all the three electrodes namely biofilm grown on CP (a), NiCP (b) and TNiCP (c). Insets show their corresponding plots of peak current vs. scan rate. It can be noted from these figures that by increasing the scan rate the redox peak current was found to be linearly increased. Besides in the case of CP, the cathodic peak was observed to flatten with increasing scan rate which may be due to instability of the protein biofilm with continuous variation of the scan rate. Unlike the biofilm on CP, the redox pair is well defined at various scan rates and the peak current was observed to increase linearly with the increment in the scan rate for the cases of biofilms grown on NiCP and TNiCP. This suggests the presence of a surface confined redox species presumably the membrane bound redox protein within the immobilized biofilm of *Acetobacter aceti*. The midpoint potential obtained in the present study matches very well with the reported values and it is attributed to the formation of PQQ-ADH complex.¹⁶ Eventually the formation of redox peak and its linear increase with the scan rate point out the fact of electron transfer between the immobilized biofilm and the electrode. Precisely, there could be an electron transfer either between the subunits of heme centers of cytochromes present within the outer cell membrane or between the redox enzymes, which are electrochemically active. Nevertheless, we have determined the rate constant value for this electron transfer process using the well-known Laviron equation derived from the dependence of redox peak current on the scan rate.²² The rate constant values for the corresponding biofilm immobilized electrodes were calculated to be 0.049 s^{-1} for CP, 0.055 s^{-1} for NiCP and 0.208 s^{-1} for TNiCP respectively. The higher value of rate constant obtained in the case of template deposited Ni indicates the possibility of a fast electron transfer process and ultimately higher catalytic current can be derived by using such electrodes as anodes for microbial fuel cells application.

3.3. SEM characterization of biofilm immobilized electrodes

Structural morphology of biofilm immobilized electrodes was further analyzed using SEM. Fig. 4 shows the SEM pictures of biofilm of *Acetobacter aceti* grown on CP (a), NiCP (b) and TNiCP (c) electrodes respectively. It is clear from these SEM pictures that all the electrodes form the pedestal area for colonizing the microorganism, namely *Acetobacter aceti*, in terms of its growth and arrangement on the electrode surface.

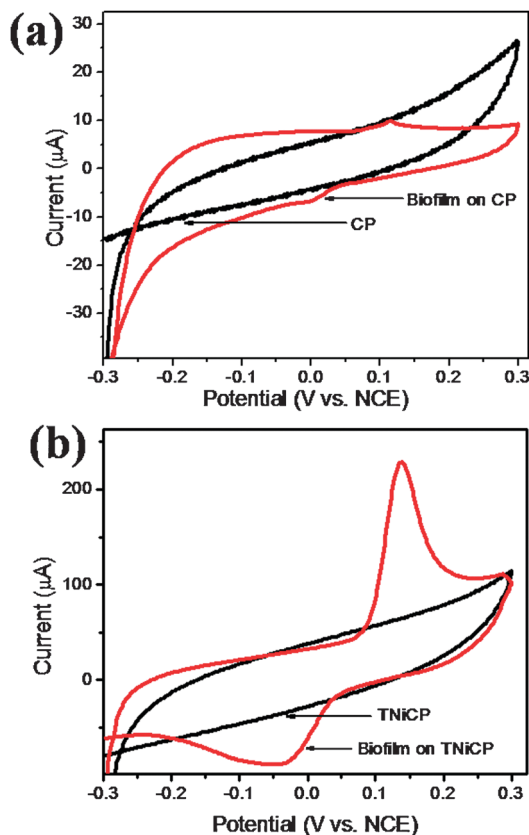


Fig. 2 Cyclic voltammograms of CP (a) and TNiCP (b) electrodes in an aqueous solution of phosphate buffer having a pH 7.0 at a potential scan rate of 50 mV s^{-1} obtained before (black line) and after (red line) the biofilm formation.

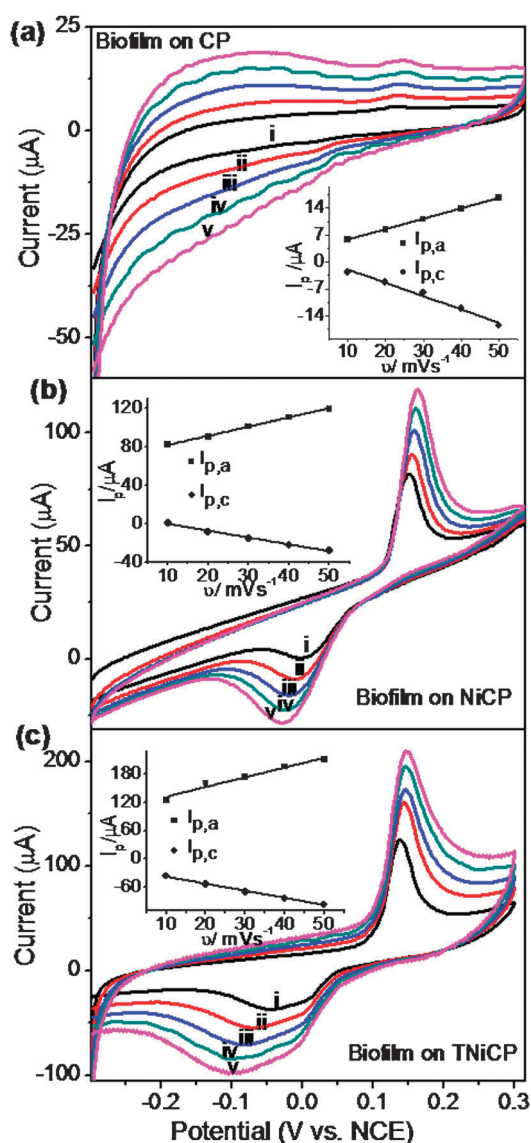


Fig. 3 Cyclic voltammograms obtained using CP (a), NiCP (b) and TNiCP (c) electrodes after the biofilm formation in phosphate buffer (pH 7.0) aqueous solution at various scan rates viz. (i) 10 mV s^{-1} , (ii) 20 mV s^{-1} , (iii) 30 mV s^{-1} , (iv) 40 mV s^{-1} and (v) 50 mV s^{-1} . Insets show their corresponding plots of redox peak current (both anodic and cathodic) vs. scan rate.

In comparison to SEM pictures obtained before microorganism growth (Fig. 1), these images clearly display the distinguishable structural features indicating the homogeneous growth of microorganism. In effect, template deposited Ni on CP exhibits a higher amount of uniform bacterial growth compared to the Ni electrode produced without the template. These results correlate very well with the surface coverage values determined for biofilm formation using CV studies discussed earlier.

3.4. Bio-electrocatalysis using glucose and ethanol as electron donors

Acetobacter aceti biofilm immobilized electrodes were investigated for their potential application as microbial anodes towards the electrocatalytic oxidation of glucose and ethanol.

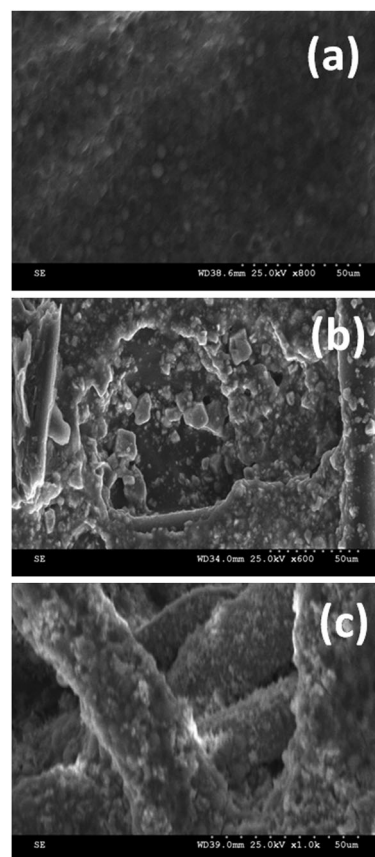


Fig. 4 SEM images of CP (a), NiCP (b) and TNiCP (c) electrodes after the biofilm formation using *Acetobacter aceti* microorganism.

CV of biofilm anchored electrodes viz., CP (a,b), NiCP (c,d) and TNiCP (e,f) was carried out in an aqueous solution of phosphate buffer (pH 7.0) at a potential sweep rate of 50 mV s^{-1} for the addition of 25 mM glucose and ethanol (Fig. 5). For comparison similar plots before the addition of electron donors were also shown for each electrode. It can be seen from these CVs that the biofilm immobilized electrodes display a redox peak formation in all the cases indicating the presence of redox species, a constituent of biofilm on the electrode surface. On adding 25 mM glucose, the oxidation current density was found to increase in the case of TNiCP when compared to CP and NiCP electrodes where the increase in oxidation current was observed to be less. A similar trend was also noted for ethanol addition. The oxidation current density of ethanol was found to be higher than the oxidation current density of glucose. Overall the TNiCP electrode exhibits a higher oxidation current density for both glucose and ethanol in comparison to other electrodes correlating well with the higher surface area and the presence of higher amounts of biofilm confirmed by our SEM and CV results discussed earlier. Moreover, the onset potential for the oxidation of glucose and ethanol in our case was found to be in the range of 0.06 to 0.09 V vs. NCE, which is lower than the potential values reported for other electrodes.^{23,24}

3.5. Application as anodes in microbial fuel cells (MFC)

Given the fact that biofilm modified electrodes of template deposited Ni oxidize effectively glucose and ethanol in neutral medium, we have evaluated the suitability of these electrodes as microbial

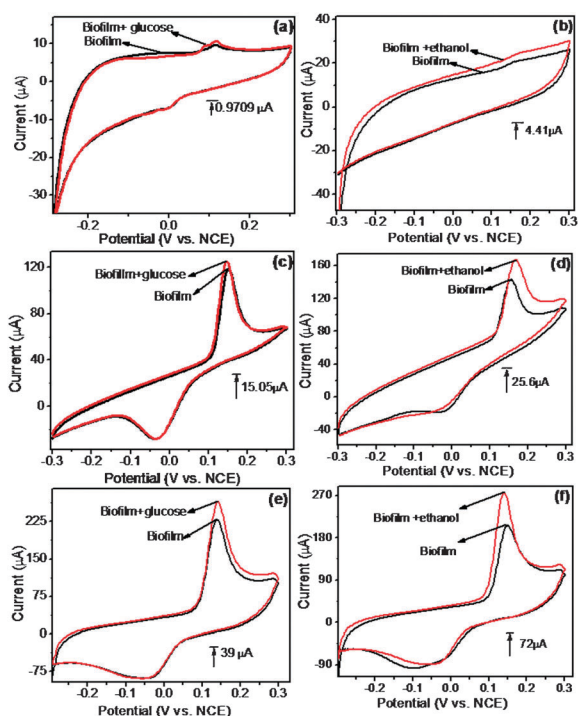
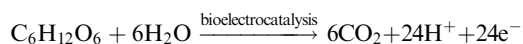


Fig. 5 CVs of biofilm of *Acetobacter aceti* immobilized electrodes namely CP (a,b), NiCP (c,d) and TNiCP (e,f) before the addition (black lines) and after the addition of glucose (25 mM) and ethanol (25 mM) (red lines) in an aqueous solution of phosphate buffer at a potential sweep rate of 50 mV s⁻¹.

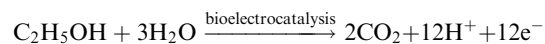
anodes in fuel cells applications through long term chronoamperometric studies. The electrodes were poised at a constant potential of 0.2 V vs. NCE and the oxidation current was monitored with respect to time. Initially the bare electrodes before the biofilm formation were kept in the phosphate buffer solution containing a 25 mM electron donor (either glucose or ethanol) and the oxidation current density was monitored for about 48 h. After that the culture inoculums were added for biofilm formation leading to attainment of the bacterial lag period. At this point the reactor solution was replaced by a fresh phosphate buffer solution (pH 7) consisting of either 25 mM glucose or ethanol (biotic process) and the oxidation current was monitored simultaneously.

In this study bare carbon paper and modified carbon electrodes were separately used as the half-cell anodes. Fig. 6(a)–(c) shows the respective chronoamperometry curves of bare CP, NiCP and TNiCP for the oxidation of glucose (25 mM). Initially the electrocatalytic activity of the anode (abiotic process) before biofilm formation and later the bio-electrocatalytic oxidation (biotic process) after the biofilm formation were investigated. The electrocatalytic current monitored before the biofilm formation was found to be insignificant when compared to bio-electrocatalytic oxidation observed after the biofilm formation towards the oxidation of glucose. The complete oxidation reaction of glucose (half-cell anode reaction) can be expressed as follows,



Based on the half cell reaction the oxidation peak current density (i_{max}) of 2.21 $\mu\text{A cm}^{-2}$ was obtained for a bare CP

electrode which is lower than the Ni deposited CP (NiCP) (36.7 $\mu\text{A cm}^{-2}$) and template Ni deposited CP (TNiCP) (42.4 $\mu\text{A cm}^{-2}$). Similarly, the chronoamperometry curves for the oxidation of ethanol (25 mM) using different electrodes namely, CP, NiCP and TNiCP, are shown in Fig. 7(a)–(c). The corresponding half-cell anode reaction is given below.



It can be seen from Fig. 6 and 7 that the oxidation current density corresponding to ethanol is significantly higher than the current density of glucose oxidation.

The maximum oxidation current density (i_{max}) measured for ethanol oxidation using the CP electrode was found to be 10.6 $\mu\text{A cm}^{-2}$ which is nearly 5 times higher than that of glucose oxidation current observed at the CP electrode (2.21 $\mu\text{A cm}^{-2}$). Similarly, the oxidation current density values of ethanol oxidation measured using NiCP (65.3 $\mu\text{A cm}^{-2}$) and TNiCP (67.6 $\mu\text{A cm}^{-2}$) were about 7 times higher than that of CP (10.6 $\mu\text{A cm}^{-2}$). It is interesting to examine the efficiency of these electrodes towards the oxidation of fuels namely glucose and ethanol in terms of their discharge capacity current over the active period of oxidation (Δt). Table 1 shows the comparison of discharge capacity per geometric area of electrode (C cm^{-2}), maximum oxidation current density (i_{max}), active period of oxidation and comparative coulombic efficiency (ϵ , %) among the three electrodes using glucose and ethanol as fuels. It can be noted from the table that the capacitive discharge of ethanol on biofilm immobilized CP (0.36 C cm^{-2}) is lower than that of glucose (1.27 C cm^{-2}) even though a higher value of i_{max} is obtained for ethanol using the same electrode. The reason may be attributed to the ability of biofilm of *Acetobacter aceti* to oxidize ethanol within the diminutive period (51 h) by forming a spike current when compared to glucose. The duration of the peak current period is less in the case of ethanol. The discharge current is maintained at the peak current for a prolonged period viz., 273 hours in the case of glucose and hence higher coulombic conversion is obtained in the case of glucose.

Discharge capacities of 3.02 C cm^{-2} (75 h) and 14.56 C cm^{-2} (138 h) were obtained for glucose oxidation using NiCP and TNiCP electrodes respectively. This clearly shows that the oxidative discharge capacity of glucose is 4.8 times higher than that of NiCP. When ethanol is used as a fuel, NiCP and TNiCP yielded the oxidative discharge capacity values of 12.25 C cm^{-2} (262 h) and 40.05 C cm^{-2} (311 h). Here the value of TNiCP is found to be nearly three times higher than that of NiCP. These results clearly reveal that template deposited Ni on CP, namely the TNiCP electrode, shows the highest values for oxidative discharge capacity, maximum current density and longer activation period compared to CP and Ni deposited CP electrodes without the template. In the case of NiCP and TNiCP electrodes the duration of the peak current is larger in the case of ethanol compared to glucose. The bioelectrocatalytic oxidation of ethanol is sustained for a longer period and hence higher coulombic conversion is obtained in the case of ethanol with NiCP and TNiCP electrodes.

The rate of biotic oxidation depends on the density of the redox moieties present on the immobilized biofilm of *Acetobacter aceti*

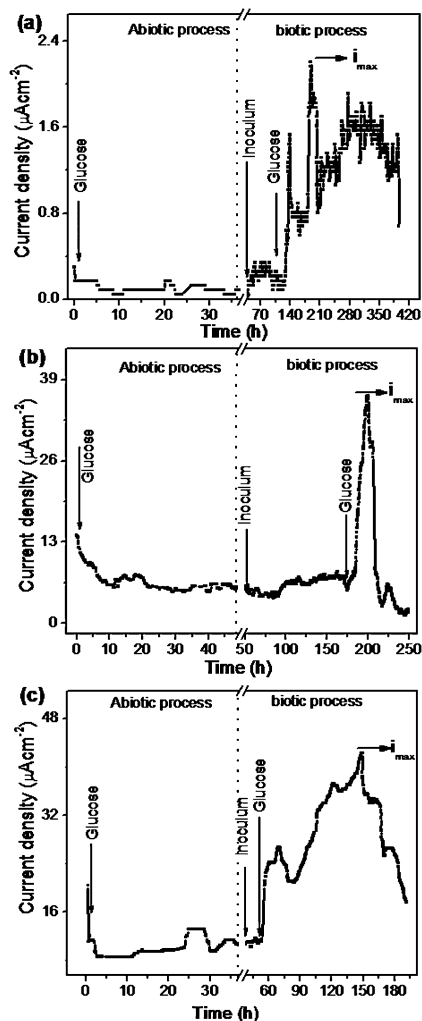


Fig. 6 Chronoamperometric graphs of *Acetobacter acetii* biofilm immobilized electrodes namely CP (a), NiCP (b) and TNiCP (c), respectively, towards glucose oxidation performed under both abiotic and biotic processes. The oxidation current density was monitored by poisoning the working electrode potential at 0.2 V *vs.* NCE using glucose as an electron donor.

which is maximum in the case of TNiCP electrodes as seen by the surface coverage values of the electroactive groups in the biofilm in Section 3.2. CV studies of the biofilm modified electrodes show the formation of redox peaks corresponding to PQQ, a cofactor of the enzyme that can be reduced to quinol form PQQH₂. Ultimately the re-oxidation of PQQH₂ takes place *via* the release of two electrons that can be transferred to the electrode surface through heme *C* units behaving as an internal mediator.

The released two electrons can reach the electrode surface *via* Ni islands present on the electrode surface. Our results clearly demonstrate the enhanced bio-electrocatalytic behaviour of *Acetobacter acetii* biofilm immobilized TNiCP electrodes towards glucose and ethanol oxidation, suggesting the potential use of these electrodes as anodes in microbial fuel cells applications. The higher activity of TNiCP arises mainly from the higher surface area and ability to incur higher amounts of bio-species on the surface, making it a better biocompatible system with improved rate constant for the direct electron transfer process.

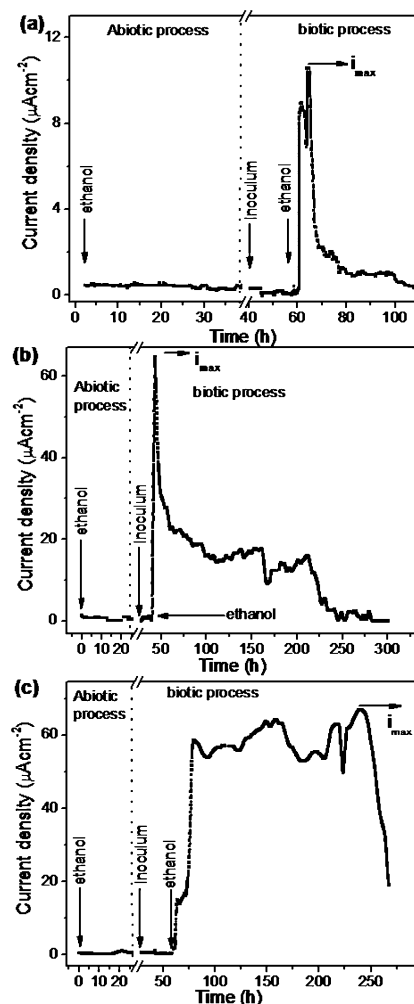


Fig. 7 Chronoamperometric plots of *Acetobacter acetii* biofilm immobilized electrodes namely CP (a), NiCP (b) and TNiCP (c), respectively, towards ethanol oxidation carried out under both abiotic and biotic processes. The oxidation current density was monitored by poisoning the working electrode potential at 0.2 V *vs.* NCE using ethanol as an electron donor.

Table 1 Maximum oxidation current density, activation period and oxidative discharge capacity obtained from chronoamperometric curves of glucose and ethanol oxidation using various electrodes namely CP, NiCP and TNiCP consisting of immobilized biofilm of *Acetobacter acetii*

Electrode	$i_{\max}/\mu\text{A cm}^{-2}$	$\Delta t/\text{hours}$	Oxidative discharge	
			capacity/C cm ⁻²	ε (%)
Glucose	CP 2.2	273	1.27	1.78
	NiCP 36.7	75	3.02	4.22
	TNiCP 42.4	138	14.56	20.36
Ethanol	CP 10.6	51	0.36	0.5
	NiCP 65.3	262	12.25	17.13
	TNiCP 67.6	311	40.05	56.01

4. Conclusions

Bio-electrochemical activity of *Acetobacter acetii* towards the oxidation of fuels such as glucose and ethanol (electron donors) was investigated using three different electrodes namely, CP, NiCP and TNiCP. From our results, we have obtained a maximum

oxidation current density of $68 \mu\text{A cm}^{-2}$ (680 mA m^{-2}) for ethanol using the TNiCP electrode. An oxidative discharge capacity of 40.05 C cm^{-2} for ethanol and 14.5 C cm^{-2} for glucose was determined using template deposited Ni on CP which are higher than that observed on NiCP and CP electrodes. This characteristic enhancement can be attributed to the electrochemically accessible area in terms of electroactive moieties per geometrical area that in the case of TNiCP was found to be $7.3763 \times 10^{-9} \text{ mol cm}^{-2}$ which is higher in comparison to NiCP and CP. The electron transfer rate constant (K_{app}) of the biofilm immobilized TNiCP electrode was estimated to be 0.2 s^{-1} which is faster than the other bio-anodes. Structural analyses of these electrodes (before and after biofilm formation) were carried out using SEM studies, which clearly shows the formation of microorganism on the electrode surface. CV studies reveal a direct electron transfer process between the immobilized biofilm of *Acetobacter aceti* and the electrode. The enhanced direct electron transfer, higher bio-electrocatalytic performance and higher oxidative discharge capacity over a longer period observed in the case of TNiCP electrode suggest that this could be used as a promising anode material for promoting direct electron transfer of *Acetobacter aceti* in microbial fuel cells applications.

Acknowledgements

The authors gratefully thank the financial support from the Ministry of New and Renewable Energy, New Delhi, India, for funding this research work (GAP 28/07). We also thank Mr K. T. Loganathan, Department of Chemistry, ACCET, Karaikudi, for his help with SEM studies.

Notes and references

- 1 D. Pant, G. V. Bogaert, L. Diels and K. Vanbroekhoven, *Bioresour. Technol.*, 2010, **101**, 1533–1543.
- 2 D. Pant, A. Singh, G. V. Bogaert, S. I. Olsen, P. S. Nigam, L. Diels and K. Vanbroekhoven, *RSC Adv.*, 2012, **2**, 1248–1263.
- 3 O. Bretschger, A. C. M. Cheung, F. Mansfeld and K. H. Nealon, *Electroanalysis*, 2010, **22**, 883–894.
- 4 L. Peng, S. J. You and J. Y. Wang, *Biosens. Bioelectron.*, 2010, **25**, 1248–1251.
- 5 Y. Qiao, C. M. Li, S. J. Bao and Q. L. Bao, *J. Power Sources*, 2007, **170**, 79–84.
- 6 Y. Qiao, S. J. Bao, C. M. Li, X. Q. Cui, Z. S. Lu and J. Guo, *ACS Nano*, 2008, **2**, 113–119.
- 7 M. Adachi, T. Shimomura, M. Komatsu, H. Yakuwa and A. Miya, *Chem. Commun.*, 2008, 2055–2057.
- 8 K. Fricke, F. Harnisch and U. Schröder, *Energy Environ. Sci.*, 2008, **1**, 144–147.
- 9 Y. Liu, F. Harnisch, K. Fricke, U. Schröder, V. Climent and J. Miguel Feliu, *Biosens. Bioelectron.*, 2010, **25**, 2167–2171.
- 10 H. J. Kim, H. S. Park, M. S. Hyun, I. S. Chang, M. Kim and B. H. Kim, *Enzyme Microb. Technol.*, 2002, **30**, 145–152.
- 11 M. Rosenbaum, F. Zhao, U. Schröder and F. Scholz, *Angew. Chem., Int. Ed.*, 2006, **45**, 6658–6661.
- 12 S. Chen, G. He, A. A. C. Martinez, S. Agarwal, A. Greiner, H. Hou and U. Schröder, *Electrochem. Commun.*, 2011, **13**, 1026–1029.
- 13 K. Matsushita, H. Toyama and O. Adachi, *Appl. Microbiol. Biotechnol.*, 2002, **58**, 13–22.
- 14 K. Matsushita, H. Toyama and O. Adachi, *Advances in microbial physiology - Respiratory chains and bioenergetics of acetic acid bacteria*, ed. A. H. Rose and D. W. Tempest, Academic, London, 1994, vol. 36, p. 247.
- 15 K. Matsushita, H. Toyama and O. Adachi, *Respiration in Archaea and Bacteria—Respiratory chains in acetic acid bacteria: Membrane-bound periplasmic sugar and alcohol respirations*, ed. D. Zannoni, Springer, Dordrecht, 2004, vol. 2, p. 81.
- 16 T. Yakushi and K. Matsushita, *Appl. Microbiol. Biotechnol.*, 2010, **86**, 1257–1265.
- 17 R. Karthikeyan, K. Sathish Kumar, M. Murugesan, S. Berchmans and V. Yegnaraman, *Environ. Sci. Technol.*, 2009, **43**, 8684–8689.
- 18 D. Pant, G. V. Bogaert, C. P. Carrero, L. Diels and K. Vanbroekhoven, *Water Sci. Technol.*, 2011, **63**, 2457–2461.
- 19 M. Chirea, V. G. Morales, J. A. Manzanares, C. Pereira, R. Gulaboski and F. Silva, *J. Phys. Chem. B*, 2005, **109**, 21808–21817.
- 20 V. Ganesh and V. Lakshminarayanan, *Electrochim. Acta*, 2004, **49**, 3561–3572.
- 21 Y. Yuan, S. Zhou, N. Xu and L. Zhuang, *Colloids Surf., B*, 2011, **82**, 641–646.
- 22 E. Laviron, *J. Electroanal. Chem.*, 1974, **52**, 355–395.
- 23 Y. F. Wang, S. S. Cheng, S. Tsujimura, T. Ikeda and K. Kano, *Bioelectrochemistry*, 2006, **69**, 74–81.
- 24 M. M. Rahman, A. J. S. Ahammad, J. H. Jin, S. J. Ahn and J. J. Lee, *Sensors*, 2010, **10**, 4855–4886.